An unified modelling of dead-zone, dead-band, hysteresis, and other faulty local behaviors of actuators and sensors

Gustave Bainier * **Benoît Marx** * **Jean-Christophe Ponsart** *

* *Université de Lorraine, CNRS, CRAN, F-54000 Nancy, France (*`gustave.bainier@univ-lorraine.fr`*)*

Abstract: Dead-zone, dead-band or hysteresis are well-known local faulty behaviors which are typically observed on the actuators and sensors of physical systems. After being identified, these local nonlinearities are usually taken into account when designing observers or controllers. This paper breaks the trend of case by case analysis of these nonlinearities, and suggest a new unifying representation which encapsulates a large class of nonlinear faults. Although more conservative than already existing specific approaches, the proposed framework necessitates very few knowledge on the nonlinearties, and may offer a practical duality between the actuator and the sensor cases. Ultimate bound guarantees are given both in the case of nonlinear and linear systems. The latter case is illustrated numerically by an example.

Keywords: Actuator fault, Sensor fault, Dead-zone, Hysteresis, Ultimate bound

1. INTRODUCTION

Nonlinear faulty local behaviors of actuators are commonly found in many physical systems, including hydraulic servovalves, electric servomotors, among other applications. Though less discussed in the literature, these faulty local behaviors can also be observed on sensors, e.g. on relative pressure sensors. These faults tend to deteriorate the controller and observer performances, sometimes even leading to instability of the whole system. Usually falling under the category of dead-zones, dead-bands or hysteresis, these types of local behaviors have been well investigated in the control literature, with an emphasis on the dead-zone of actuators [Tao and Kokotovic, 1996, Tao and Lewis, 2001].

Two primary approaches are commonly used to mitigate the impact of dead-zones [Gianino, 1994]. The first method is to implement an active compensation control strategy on the actuators based on a dead-zone inverse [Tao and Kokotovic, 1994]: this method is however limited since the inverse is discontinuous, and it does not exist if the dead-zone is in fact a dead-band (Figure 1), or if it affects a sensor. The second approach models the dead-zone as a combination of a linear control input with a constant or time-varying gain and a bounded disturbance-like term. This disturbance-like term is typically treated as an uncertain nonlinearity and is handled using robust feedback mechanisms [Zhang et al., 2014]. This paper extends the second approach, allowing the modelling of a broader range of nonlinear local behaviors.

Also very much investigated in the control literature from a theoretical point of view, a lot of models of hysteresis have been developed over the years for control purposes, including - among others - the Preisach model [Preisach, 1935], the Duhem model [Duhem, 1897] and its variations (e.g. the Bouc-Wen, LuGre, Dahl models...). The reader is referred to [Hassani et al., 2014] for more details.

In this paper, a new unifying representation which encapsulates the nonlinearities discussed above is proposed, leading to ultimate bound guarantees both in the case of nonlinear and linear systems. Even if the suggested framework is more conservative compared to pre-existing specialized methods, it nevertheless requires minimal knowledge of nonlinearities, and moreover establishes a duality between the actuators and sensors local nonlinearities.

This paper is organized as follows: Sections 2 and 3 introduce respectively the notations used in the paper and some preliminary results. In Section 4, the unified modelling of faulty local nonlinear behaviors on actuators and sensors is introduced. Early ultimate bounds results for Linear Time Invariant (LTI) systems are provided in Section 5, and these results are applied on a simple example in Section 6. Finally, Section 7 concludes the paper.

2. DEFINITIONS, NOTATIONS

The set of integers between a and b (both included) is denoted $[\![a, b]\!]$. The i-th coordinate of a vector $v \in \mathbb{R}^n$ is denoted $v_{(i)}$. Given $P = P^\top$ a real symmetric matrix, $\lambda_{\max}(P)$ (resp. $\lambda_{\min}(P)$) stands for the largest (resp. smallest) eigenvalue of P. Moreover, $\preceq$ ($\prec$) stands for the (strict) Loewner order. The definitions of a ball and of an ellipsoid of $\mathbb{R}^n$ centered at the origin are recalled below

$$\mathcal{B}(r) \triangleq \{x \in \mathbb{R}^n : \|x\|_2 \leqslant r\} \tag{1}$$

$$\mathcal{E}(Q, r) \triangleq \{x \in \mathbb{R}^n : \sqrt{x^\top Q x} \leqslant r\} \tag{2}$$

In (2), usually $Q = Q^\top \succ 0$, but this paper tolerates $Q = Q^\top \succeq 0$, which provides a degenerate ellipsoid. Moreover,

$\mathcal{B} \triangleq \mathcal{B}(1)$ and $\mathcal{E}(Q) \triangleq \mathcal{E}(Q,1)$. Given a set $S \subseteq \mathbb{R}^n$, $\mathbf{1}_S$ stands for the indicator function $\mathbf{1}_S(x) \triangleq 1$ if $x \in S, 0$ else.

3. PRELIMINARY RESULTS

Lemma 1. For all $\beta, \eta > 0$, the following inequality holds:

$$\mathbf{1}_{\mathcal{B}} \leqslant \exp\left[\beta(1 - \|\cdot\|_2^{\eta})\right] \tag{3}$$

moreover the following limit is verified

$$\lim_{m\to\infty} \exp\left[\frac{1}{m}(1 - \|\cdot\|_2^{m})\right] = \mathbf{1}_{\mathcal{B}} \text{ pointwise} \tag{4}$$

but this convergence is non-uniform.

Proof. Let $x \in \mathbb{R}^n$. If $x \notin \mathcal{B}$, then $\exp\left[\beta(1 - \|x\|_2^{\eta})\right] \geqslant 0$ is obvious. Moreover, $\|x\|_2 > 1$, hence $\lim_{m\to\infty} \frac{1}{m}(1 - \|x\|_2^{m}) = -\infty$, providing (4) for such x. If $x \in \mathcal{B}$, then $\|x\|_2 \leqslant 1$ and $\exp\left[\beta(1 - \|x\|_2^{\eta})\right] \geqslant e^0 = 1$. Moreover, $\lim_{m\to\infty} \frac{1}{m}(1 - \|x\|_2^{m}) = 0$, again providing (4) for such x. Finally, the convergence (4) cannot be uniform since $\exp\left[\frac{1}{m}(1 - \|\cdot\|_2^{m})\right]$ is continuous on $\mathbb{R}^n$ for all m, whereas $\mathbf{1}_{\mathcal{B}}$ is discontinuous. □

Lemma 2. (Minimum-volume covering ellipsoid). Given a set $\mathcal{S} \subset \mathbb{R}^n$, the minimum volume ellipsoid $\mathcal{E}(M^\top M)$ centered at the origin and covering $\mathcal{S}$ is found with the optimization problem (5).

$$\begin{aligned} M = \arg\min_{M>0} & (-\log\det M) \\ \text{s.t. } & (Mx)^\top Mx \leqslant 1, \quad \text{for all } x \in \mathcal{S} \end{aligned} \tag{5}$$

In particular, this problem is convex when $\mathcal{S}$ is the convex hull of a finite set [Sun and Freund, 2004].

Lemma 3. (Radius of the intersection of ellipsoids). Given m (eventually degenerated) ellipsoids $\mathcal{E}(Q_i, r_i)$ and $Q_0 = Q_0^\top > 0$, with for all $i = 1, \dots, m$, $Q_i = Q_i^\top \geq 0$, if a minimal radius $r_0 > 0$ exists such that

$$\bigcap_{i=1}^{m} \mathcal{E}(Q_i, r_i) \subseteq \mathcal{E}(Q_0, r_0) \tag{6}$$

then r_0 is given by

$$\begin{aligned} r_0^2 = \max_{x\in\mathbb{R}^n} & \; x^\top x \\ \text{s.t. } & x^\top T_i x \leqslant r_i^2, \text{ for all } i = 1, \dots, m \end{aligned} \tag{7}$$

with $T_i \triangleq Q_0^{-\frac{1}{2}\top} Q_i Q_0^{-\frac{1}{2}}$. However, this problem is concave, and there are no efficient numerical procedures to solve it exactly. This paper uses the following "rank 1 dropping" Semidefinite Programming (SDP) relaxation to upper-bound the minimal radius:

$$\begin{aligned} r_0^2 \leqslant \max_{X=X^\top\geq 0} & \; \operatorname{Tr} X \\ \text{s.t. } & \operatorname{Tr}(T_i X) \leqslant r_i^2, \text{ for all } i = 1, \dots, m \end{aligned} \tag{8}$$

The reader is referred to [Henrion et al., 1998] for a review on the subject, including (8) among other convex relaxations of (7).

4. A GENERALIZED MODEL OF ACTUATORS DEAD-ZONE, DEAD-BAND AND HYSTERESIS

Consider the nonlinear system

$$\begin{cases} \dot{x}(t) = f\left(x(t), \tilde{u}(t)\right) \\ \tilde{u}(t) = h(u(t)) \end{cases} \tag{9}$$

with $x(t) \in \mathbb{R}^{n_x}$ the state of the system, $\tilde{u}(t) \in \mathbb{R}^{n_u}$ its control input and $u(t) \in \mathbb{R}^{n_u}$ the reference signal

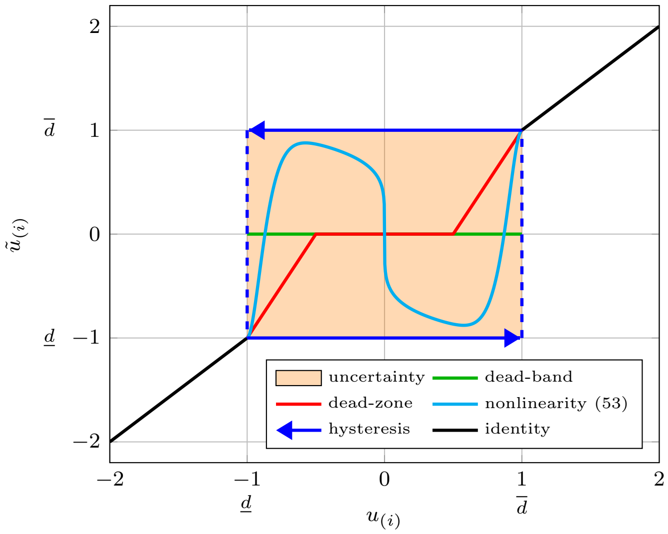

Fig. 1. Nonlinear local behaviors of actuators, and their suggested unified uncertain modelling, $\overline{d} = -\underline{d} = 1$

given to the actuators. From now on, the time dependence is omitted for concision. The function f is continuously differentiable and globally Lipschitz in $(x, \tilde{u})$, and h is a nonlinear function modelling the nonlinear faults affecting the actuators, such as their dead-zone, dead-band or hysteresis. In this paper, instead of specifying exactly h, the authors suggest a generic expression for h of the form

$$\tilde{u} = h(u) = u + \delta \tag{10}$$

where $\delta \in \mathbb{R}^{n_u}$ is considered to be an unknown piecewise continuous signal. This allows h to model a wide range of nonlinear actuator faults without precise knowledge on them. The assumptions made on δ differ depending on whether the actuators nonlinear faults affect $\tilde{u}$ component-wise or not. In both cases, two vectors $\overline{d}$ and $\underline{d}$ of $\mathbb{R}^{n_u}$ are defined such that $\underline{d}_{(i)} < 0 < \overline{d}_{(i)}$ for $i = 1, \dots, n_u$.

4.1 Local component-wise nonlinearities

If each coordinate of the control input vector $\tilde{u}_{(i)}$ is subject to a nonlinear distortion with respect to the nominal signal $u_{(i)}$ for $u_{(i)} \in [\underline{d}_{(i)}, \overline{d}_{(i)}]$, then h is nonlinear in the following domain:

$$\mathcal{D}_u \triangleq \left\{ u \in \mathbb{R}^{n_u} : \exists i \in [\![1, n_u]\!] \text{ s.t. } u_{(i)} \in [\underline{d}_{(i)}, \overline{d}_{(i)}] \right\} \tag{11}$$

Outside of $\mathcal{D}_u$, h is considered to be the identity function. It is moreover assumed that this input distortion remains bounded according to the following property:

$$u_{(i)} \in [\underline{d}_{(i)}, \overline{d}_{(i)}] \Rightarrow \tilde{u}_{(i)} \in [\underline{d}_{(i)}, \overline{d}_{(i)}] \tag{12}$$

Usual candidates for h satisfying these properties include the dead-band:

$$[h(u)]_{(i)} = 0 \quad \text{if } u_{(i)} \in [\underline{d}_{(i)}, \overline{d}_{(i)}] \tag{13}$$

the continuous dead-zone:

$$[h(u)]_{(i)} = \begin{cases} \dfrac{\underline{d}_{(i)}}{\underline{d}_{(i)} - \underline{\varepsilon}_{(i)}}(u_{(i)} - \underline{\varepsilon}_{(i)}) & \text{if } \underline{d}_{(i)} \leqslant u_{(i)} < \underline{\varepsilon}_{(i)} \\ 0 & \text{if } \underline{\varepsilon}_{(i)} \leqslant u_{(i)} \leqslant \overline{\varepsilon}_{(i)} \\ \dfrac{\overline{d}_{(i)}}{\overline{d}_{(i)} - \overline{\varepsilon}_{(i)}}(u_{(i)} - \underline{\varepsilon}_{(i)}) & \text{if } \overline{\varepsilon}_{(i)} < u_{(i)} \leqslant \overline{d}_{(i)} \end{cases} \tag{14}$$

with $\underline{d}_{(i)} < \underline{\varepsilon}_{(i)} < 0 < \overline{\varepsilon}_{(i)} < \overline{d}_{(i)}$ for $i = 1, \ldots, n_u$, or even the Preisach hysteresis [Preisach, 1935]:

$$[h(u)]_{(i)} = \text{"last value of } u_{(i)} \text{ outside of } [\underline{d}_{(i)}, \overline{d}_{(i)}]\text{"} \quad (15)$$

Instead of choosing one of the representation above, (10) is preferred, with the unknown signal δ satisfying:

$$\begin{cases} \delta_{(i)} \in [\underline{d}_{(i)} - u_{(i)}, \overline{d}_{(i)} - u_{(i)}] & \text{if } u_{(i)} \in [\underline{d}_{(i)}, \overline{d}_{(i)}] \\ \delta_{(i)} = 0 & \text{else} \end{cases} \quad (16)$$

It is easily verified that the dead-zone, dead-band and hysteresis described above can all be embedded in this representation (Figure 1). Moreover, it is also easily verified that δ is bounded inside a set D defined by:

$$D \triangleq [\underline{d}_{(1)} - \overline{d}_{(1)}, \overline{d}_{(1)} - \underline{d}_{(1)}] \times \cdots \times [\underline{d}_{(n_u)} - \overline{d}_{(n_u)}, \overline{d}_{(n_u)} - \underline{d}_{(n_u)}] \quad (17)$$

hence $\|\delta\|_2 \leqslant \|\overline{d} - \underline{d}\|_2$, where $\times$ denotes the Cartesian product of sets. Note that in the case of a dead-zone, this modelling can be leveraged after applying a first approximate "smooth dead-zone inverse" to the reference input signal, hence reducing the conservatism of the assumptions of this section.

4.2 Local nonlinearities of $\mathbb{R}^{n_u}$

Although very rarely discussed in the dead-zone literature, some local actuators faults may lead to a distortion of $\tilde{u}$ with respect to its nominal signal u which is restricted to a bounded set surrounding the origin of the input space $\mathbb{R}^{n_u}$. In that case, h can be considered nonlinear in an orthotopic domain $\mathcal{D}_u^{\square}$ defined by:

$$\mathcal{D}_u^{\square} \triangleq \left\{ u \in \mathbb{R}^{n_u} : \forall i \in [\![1, n_u]\!], \, u_{(i)} \in [\underline{d}_{(i)}, \overline{d}_{(i)}] \right\} \quad (18)$$

Outside of $\mathcal{D}_u^{\square}$, h is considered to be the identity function. Again, it is assumed that this input distortion remains bounded according to the following property:

$$u \in \mathcal{D}_u^{\square} \Rightarrow \tilde{u} \in \mathcal{D}_u^{\square} \quad (19)$$

These kind of local nonlinearities are typically found on actuators with several degree of freedom, e.g. radial dead-zones of joysticks [Goel et al., 2003, Ding et al., 2004]. They are usually purposefully imposed to physical systems in order to avoid over-sensitivity of the system to small input values, but it is nonetheless useful to study their effect [Broschart and Scheeres, 2007]. Moreover, even if the nonlinearities of the actuators are actually component-wise, the assumptions of this section can be leveraged as an intermediary step in order to diminish the overall conservatism of the study (see Corollary 9).

It is easily verified that $\delta \in D = (17)$ still holds true here. Moreover, a practical upper-bounding to $\|\delta\|_2$ in that case is given by the following Lemma.

Lemma 4. Given $\mathcal{E}(M^\top M)$ an ellipsoid centered at the origin and covering $\mathcal{D}_u^{\square}$ (obtained through Lemma 2), then for all $\beta, \eta > 0$, the following upper-bound holds:

$$\|\delta(u)\|_2 \leqslant \|\overline{d} - \underline{d}\|_2 \exp\left[\beta\left(1 - \|Mu\|_2^{\eta}\right)\right] \quad (20)$$

Proof. For all $u \notin \mathcal{D}_u^{\square}$, $\|\delta(u)\|_2 = 0$; and for all $u \in \mathcal{D}_u^{\square}$,

$$\|\delta(u)\|_2 \leqslant \|\overline{d} - \underline{d}\|_2$$

The minimum-volume ellipsoid centered at the origin covering $\mathcal{D}_u^{\square}$ provides:

$$\|\delta(u)\|_2 \leqslant \|\overline{d} - \underline{d}\|_2 \mathbf{1}_{\mathcal{B}}(Mu) \quad (21)$$

and (20) is obtained with Lemma 1. □

4.3 A generic ultimate bound guarantee

The nonlinear system (9) can be re-written by considering δ as a new unknown input

$$\dot{x} = f_a(x, u, \delta) \quad (= f(x, u + \delta)) \quad (22)$$

with f_a a continuously differentiable and globally Lipschitz function in (x, u, δ). Given a state feedback reference signal, the next result provides a simple condition to guarantee the ultimate boundedness of the closed-loop system, no matter if the nonlinearities of the actuators act on the control input component-wise or not.

Theorem 5. (Ultimate boundedness). If there exists a state feedback law $u = g(x)$ with g continuously differentiable and globally Lipschitz in x such that

$$\dot{x} = f_a(x, g(x), 0) \quad (23)$$

has a globally exponentially stable equilibrium at $x = 0$, then for all bounded signal $\delta \in D = (17)$, there exists $r > 0$ such that for all initial state $x_0 \in \mathbb{R}^{n_x}$, the state trajectory x of (22) taken with $u = g(x)$ is ultimately bounded by $\mathcal{B}(r)$.

Proof. From Lemma 4.5 page 108 of [Khalil, 2014], (22) with $u = g(x)$ is Input-to-State Stable in δ. In particular, by an application of Definition 4.4 page 107 of [Khalil, 2014] for all initial state $x_0 \in \mathbb{R}^{n_x}$, the state trajectory x is ultimately bounded by

$$\gamma\left(\sup_{t_0 \leqslant \tau \leqslant t} \|\delta(\tau)\|_2\right) \leqslant \gamma\left(\sup_{\delta \in D} \|\delta\|_2\right) \leqslant \gamma\left(\|\overline{d} - \underline{d}\|_2\right) \quad (24)$$

with γ a class $\mathcal{K}$ function. In other words, there exists $r > 0$ such that for all x_0, there exists a $T > 0$ providing $x(t) \in \mathcal{B}(r)$ for all $t \geqslant t_0 + T$. □

4.4 Duality regarding sensors

Contrary to actuators, dead-zone of sensors are not theoretically invertible. Instead, the output $\tilde{y} \in \mathbb{R}^{n_y}$ of sensors subject to faults like dead-zone, dead-band or hysteresis becomes uncertain when measured in a specific range of values. By making similar assumptions as previously, a system subject to local nonlinear sensor faults may be written using an unknown signal δ:

$$\begin{cases} \dot{x} = f(x) \\ \tilde{y} = h(y) = y + \delta \end{cases} \quad \text{with } \delta \in D = (17) \quad (25)$$

with $y \in \mathbb{R}^{n_y}$ the theoretical value that the sensors should measure. This symmetry of assumptions between the nonlinear actuator and sensor faults allowed by our simple modelling is not usual in the dead-zone literature, although it allows to very easily generalize the ultimate bounds discussed in the next section to the observer design problem, by duality between the linear state feedback control laws and the Luenberger observers.

5. ULTIMATE BOUND FOR LTI SYSTEMS

Given a stabilizable LTI system (26) subject to local nonlinear actuator faults, this section establishes ultimate bound guarantees on an usual linear state-feedback control $u = Kx$ with an imposed decay-rate $\alpha > 0$.

$$\begin{cases} \dot{x} = Ax + B\tilde{u} \\ \tilde{u} = h(u) = u + \delta \end{cases} \quad \text{with } \delta \in D = (17) \quad (26)$$

It is assumed there exists a gain matrix K and a symmetric positive definite matrix $P = P^\top > 0$ such that the following holds:

$$(A + BK)^\top P + P(A + BK) \preceq -2\alpha P \tag{27}$$

meaning the control law $u = Kx$ imposes a minimum decay rate $\alpha > 0$ to the nominal closed-loop system $\dot{x} = (A + BK)x$.

Theorem 6. (Generic ultimate bound). System (26) associated with the control law $u = Kx$ such that (27) holds is ultimately bounded by $\mathcal{E}(P, r)$ with

$$r = \frac{\sqrt{\lambda_{\max}(P)}}{\alpha\lambda_{\min}(P)}\|PB\|_2 \left\|\overline{d} - \underline{d}\right\|_2 \tag{28}$$

Proof. It is easily obtained from (27) that the derivative of the Lyapunov function $V(x) = x^\top Px$ along the trajectories of (26) with $u = Kx$ respects:

$$\begin{aligned}\dot{V}(x) &\leqslant -2\alpha x^\top Px + 2x^\top PB\delta \\ &\leqslant -2\alpha\lambda_{\min}(P)\|x\|_2^2 + 2\|x\|_2\|PB\|_2\|\delta\|_2\end{aligned} \tag{29}$$

Thus, $\dot{V}(x) < 0$ is verified when

$$\|x\|_2 > \frac{\|PB\|_2\|\delta\|_2}{\alpha\lambda_{\min}(P)} \tag{30}$$

hence, the ultimate bound of the system can be computed as the following level-set:

$$V(x) = \lambda_{\max}(P)\left(\frac{\|PB\|_2\|\delta\|_2}{\alpha\lambda_{\min}(P)}\right)^2 \tag{31}$$

and the inequality $\|\delta\|_2 \leqslant \left\|\overline{d} - \underline{d}\right\|_2$ concludes the proof. ▫

The result discussed above holds whether the distortion of the input is component-wise or not. However, because it does not take into account the dependency between the uncertainties δ and the state of the system x, this ultimate bound is rather conservative. Other ultimate bounds are suggested below, both when the nonlinear fault affecting $\tilde{u}$ is component-wise or not.

In order to deal with the component-wise case of Section 4.1, where h is nonlinear on $\mathcal{D}_u = (11)$, the set of indices (32) is introduced to list which coordinates of δ are active (i.e. not zero) at a given state x.

$$\mathcal{I}(x) \triangleq \left\{i \in [\![1, n_u]\!] : \underline{d}_{(i)} \leqslant (Kx)_{(i)} \leqslant \overline{d}_{(i)}\right\} \tag{32}$$

Moreover, for each non-empty subset $\mathcal{J} \subseteq [\![1, n_u]\!]$, the polytope (33) is defined under a half-space representation as follows:

$$\mathcal{P}_{\mathcal{J}} \triangleq \left\{ x \in \mathbb{R}^{n_x} : \begin{cases} \mathcal{J} \subseteq \mathcal{I}(x) \\ \|x\|_\infty \leqslant a\sqrt{\sum_{j\in\mathcal{J}}\left(\overline{d}_{(j)} - \underline{d}_{(j)}\right)^2} \end{cases} \right\}$$
$$\text{with } a = \frac{\|PB\|_2}{\alpha\lambda_{\min}(P)} \tag{33}$$

note that $\mathcal{J} \subseteq \mathcal{I}(x)$ is verified for all $x \in \mathbb{R}^{n_x}$ such that:

$$\forall j \in \mathcal{J},\ \underline{d}_{(j)} \leqslant (Kx)_{(j)} \leqslant \overline{d}_{(j)} \tag{34}$$

Theorem 7. (Component-wise ultimate bound). If $\delta \in D = (17)$ follows the assumptions of Section 4.1, system (26) associated with the control law $u = Kx$ such that (27) holds is ultimately bounded by $\mathcal{E}(P, r)$ with

$$\begin{aligned} r^2 = &\max_{x\in\mathbb{R}^n}\ x^\top Px \\ &\text{s.t. } x \in \bigcup_{\mathcal{J}\subseteq[\![1,n_u]\!]} \mathcal{P}_{\mathcal{J}} \end{aligned} \tag{35}$$

which can be computed by enumerating the vertices of all the polytopes $\mathcal{P}_{\mathcal{J}} = (33)$.

Proof. Similarly to the proof of Theorem 6, for $V(x) = x^\top Px$, $\dot{V}(x) < 0$ is verified when

$$\|x\|_2 > \frac{\|PB\|_2\|\delta\|_2}{\alpha\lambda_{\min}(P)} \tag{36}$$

in particular, if $\|x\|_\infty > a\|\delta\|_2$ then $\dot{V}(x) < 0$ holds, with a defined in (33). Since for all $i \notin \mathcal{I}(x)$, $\delta_{(i)} = 0$, it follows that if $\mathcal{I}(x) = \varnothing$ then $\|\delta\|_2 = 0$, and if $\mathcal{I}(x) \neq \varnothing$ then

$$\|\delta\|_2^2 = \sum_{i\in\mathcal{I}(x)} \delta_{(i)}^2 \leqslant \sum_{i\in\mathcal{I}(x)} \left(\overline{d}_{(i)} - \underline{d}_{(i)}\right)^2 \tag{37}$$

Reciprocally, if $\dot{V}(x) \geqslant 0$, then $\|x\|_\infty \leqslant a\|\delta\|_2$, and either $\mathcal{I}(x) = \varnothing$ hence $x = 0$, or there exists $\mathcal{J} \subseteq [\![1, n_u]\!]$ such that $\mathcal{J} \subseteq \mathcal{I}(x)$ and $\|x\|_\infty \leqslant a\sqrt{\sum_{i\in\mathcal{J}}(\overline{d}_{(i)} - \underline{d}_{(i)})^2}$. This provides that $\dot{V}(x)$ can only be positive for x inside a polytope $\mathcal{P}_{\mathcal{J}}$, which is to say $\dot{V}(x) < 0$ for all $x \notin \bigcup_{\mathcal{J}\subseteq[\![1,n_u]\!]} \mathcal{P}_{\mathcal{J}}$. In the end, the ultimate bound of the system can be computed as the smallest level-set of V containing $\bigcup_{\mathcal{J}\subseteq[\![1,n_u]\!]} \mathcal{P}_{\mathcal{J}}$, i.e. through the optimization problem (35). ▫

A similar reasoning can be carried out when δ follows the assumptions of Section 4.2, where h is nonlinear on $\mathcal{D}_u^\square = (18)$, by enumerating the vertices of the polytope $\mathcal{P}_{[\![1,n_u]\!]}$ directly.

Keeping the assumptions of Section 4.2, the next result leverages the upper-bound of Lemma 4 in order to obtain an ultimate bound through a simple SDP optimization problem.

Theorem 8. (Non component-wise ultimate bound). If $\delta \in D = (17)$ follows the assumptions of Section 4.2, system (26) associated with the control law $u = Kx$ such that (27) holds is ultimately bounded by $\mathcal{E}(P, r)$ with

$$\begin{aligned} r^2 = &\max_{X=X^\top\succeq 0}\ \operatorname{Tr} X \\ &\text{s.t. } \operatorname{Tr}(T_iX) \leqslant r_i^2, \text{ for } i = 1, 2 \end{aligned} \tag{38}$$

where

$$T_1 \triangleq P^{-\frac{1}{2}\top} R \begin{bmatrix} I_p & 0 \\ 0 & 0 \end{bmatrix} R^\top P^{-\frac{1}{2}} \tag{39}$$

$$T_2 \triangleq P^{-\frac{1}{2}\top} R \begin{bmatrix} 0 & 0 \\ 0 & I_{n_x-p} \end{bmatrix} R^\top P^{-\frac{1}{2}} \tag{40}$$

$$r_1 \triangleq \frac{\left[W_0\left(\eta\beta\lambda_{\min}^{\eta/2}(\Lambda)r_2^\eta\right)/\eta\beta\right]^{\frac{1}{\eta}}}{\lambda_{\min}^{1/2}(\Lambda)} \tag{41}$$

$$r_2 \triangleq \frac{\|PB\|_2}{\alpha\lambda_{\min}(P)} \left\|\overline{d} - \underline{d}\right\|_2 e^\beta \tag{42}$$

where W_0 denotes the principal branch of the Lambert W function, R is a unitary matrix such that $\lambda_{\min}(\Lambda) > 0$ in

$$K^\top QK = R\operatorname{diag}(\lambda_1, \ldots, \lambda_p, 0, \ldots, 0)R^\top = R\begin{bmatrix} \Lambda & 0 \\ 0 & 0 \end{bmatrix} R^\top \tag{43}$$

and $Q \triangleq M^\top M$, with M provided by Lemma 4.

Proof. Similarly to the proof of Theorem 6, for $V(x) = x^\top P x$, $\dot{V}(x) < 0$ is verified when

$$\|x\|_2 > \frac{\|PB\|_2 \|\delta\|_2}{\alpha \lambda_{\min}(P)} \tag{44}$$

leveraging the upper-bound (20) of Lemma 4, $\dot{V}(x) < 0$ stands for all x such that:

$$\|x\|_2 > \frac{\|PB\|_2}{\alpha \lambda_{\min}(P)} \left\|\overline{d} - \underline{d}\right\|_2 \exp\left[\beta\left(1 - (u^\top Q u)^{\frac{\eta}{2}}\right)\right] \tag{45}$$

i.e.

$$\|x\|_2 \exp\left[\beta(x^\top K^\top Q K x)^{\frac{\eta}{2}}\right] > r_2 \tag{46}$$

$K^\top Q K$ is real-symmetric hence unitary diagonalizable. We take $x = Rz = R\begin{bmatrix} z_1^\top & z_2^\top \end{bmatrix}^\top$, with R a unitary matrix and such that (43) holds. This provides $\dot{V}(x) < 0$ for all z such that:

$$\sqrt{(Rz)^\top Rz} \exp\left[\beta(z_1^\top \Lambda z_1)^{\frac{\eta}{2}}\right] > r_2 \tag{47}$$

note that since R is unitary, $R^\top R = I_{n_u}$ follows, hence $\dot{V}(x) < 0$ holds if:

$$\sqrt{(z_1^\top z_1 + z_2^\top z_2) \exp\left[2\beta(z_1^\top \Lambda z_1)^{\frac{\eta}{2}}\right]} > r_2 \tag{48}$$

which also holds, since $2\beta(z_1^\top \Lambda z_1)^{\frac{\eta}{2}} \geqslant 0$, if:

$$\sqrt{z_1^\top z_1 \exp\left[2\beta(z_1^\top \Lambda z_1)^{\frac{\eta}{2}}\right] + z_2^\top z_2} > r_2 \tag{49}$$

Finally $\dot{V}(x) < 0$ holds if:

$$\max\left\{\|z_1\|_2 \exp\left[\beta \lambda_{\min}^{\eta/2}(\Lambda)\|z_1\|_2^\eta\right], \|z_2\|_2\right\} > r_2 \tag{50}$$

In particular for z_1:

$$\begin{aligned} &\|z_1\|_2 \exp\left[\beta \lambda_{\min}^{\eta/2}(\Lambda)\|z_1\|_2^\eta\right] > r_2 \\ \Leftrightarrow\ &\|z_1\|_2 > \frac{\left[W_0\left(\eta\beta\lambda_{\min}^{\eta/2}(\Lambda) r_2^\eta\right)/\eta\beta\right]^{\frac{1}{\eta}}}{\lambda_{\min}^{1/2}(\Lambda)} = r_1 \end{aligned} \tag{51}$$

In the end, the ultimate bound of the system can be computed as the smallest level-set of V containing the intersection of the two degenerate ellipsoids $\|z_1\|_2 < r_1$ and $\|z_2\|_2 < r_2$, and Lemma 3 provides the tractable optimization problem (38) to obtain this level-set. □

This ultimate bound can actually be leveraged with a $\delta \in D = (17)$ following the assumptions of Section 4.1 if a sufficiently small ultimate bound is already known.

Corollary 9. If $\delta \in D = (17)$ follows the assumptions of Section 4.1, system (26) associated with the control law $u = Kx$ such that (27) holds is ultimately bounded by $\mathcal{E}(P, r_1)$ with r_1 defined by (38) if there exists $r_2 > r_1$ such that $\mathcal{E}(P, r_2) \subset \mathcal{X}$ with $\mathcal{E}(P, r_2)$ an ultimate bound for the system and $\mathcal{X}$ defined by

$$\mathcal{X} \triangleq \{x \in \mathbb{R}^{n_x} : Kx \in \mathcal{D}_u^\square = (18)\} \tag{52}$$

Proof. For all $x \in \mathcal{X}$, the assumptions on δ of Section 4.1 and of Section 4.2 are equivalent. Hence $\dot{V}(x) < 0$ holds for all $x \notin \mathcal{E}(P, r_2)$ and for all $x \in \mathcal{X} \backslash \mathcal{E}(P, r_1)$. Since $\mathcal{E}(P, r_2) \subset \mathcal{X}$, overall, $\dot{V}(x) < 0$ for all $x \notin \mathcal{E}(P, r_1)$, which concludes the proof. □

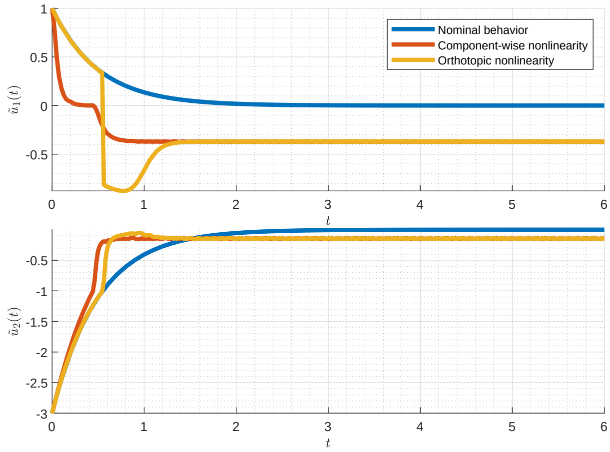

Fig. 2. Closed-loop input $\tilde{u}(t)$

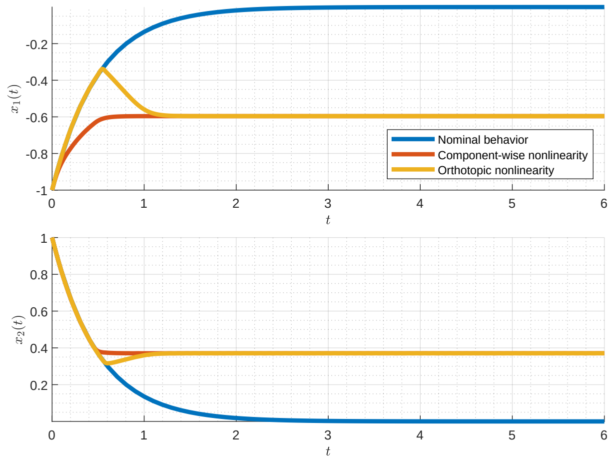

Fig. 3. Closed-loop state $x(t)$

6. APPLICATION

The results of the previous section are applied to (26) taken with $A = \begin{bmatrix} 0 & 1 \\ 1 & 2 \end{bmatrix}$, $B = I_2$, and $K = \begin{bmatrix} -2 & -1 \\ -1 & -4 \end{bmatrix}$. It is easily verified that (27) holds with $\alpha = 2$, $P = I_2$. Moreover, the vectors $\overline{d}, \underline{d} \in \mathbb{R}^2$ are defined by $\overline{d}_{(i)} = -\underline{d}_{(i)} = 1, i = 1, 2$. In simulation (Figures 2, 3, 4), the nonlinear function h is taken such that (53) holds on $\mathcal{D}_u = (11)$ and $\mathcal{D}_u^\square = (18)$ respectively (Figure 1).

$$\tilde{u}_{(i)} = h(u_{(i)}) = -\text{sign}(u_{(i)})|u_{(i)}|^{\frac{1}{5}} \cos(\pi u_{(i)}^5) \tag{53}$$

6.1 Component-wise nonlinearity

A simple application of Theorem 6 provides $\|x\|_2 \leqslant \sqrt{2} = \text{UB}_1$ as a first ultimate bound of the system. Moreover, applying Theorem 7 with

$$\mathcal{P}_{\{1\}} = \left\{x \in \mathbb{R}^2 : \max\left\{|2x_1 + x_2|, \|x\|_\infty\right\} \leqslant 1\right\} \tag{54}$$

$$\mathcal{P}_{\{2\}} = \left\{x \in \mathbb{R}^2 : \max\left\{|x_1 + 4x_2|, \|x\|_\infty\right\} \leqslant 1\right\} \tag{55}$$

$$\mathcal{P}_{\{1,2\}} = \left\{x \in \mathbb{R}^2 : \max\left\{\begin{matrix} |2x_1 + x_2|, \\ |x_1 + 4x_2|, \\ \|x\|_\infty/\sqrt{2} \end{matrix}\right\} \leqslant 1\right\} \tag{56}$$

provides the norm of the vertex $\mathcal{V} = \begin{bmatrix} -1 & 1 \end{bmatrix}^\top$ as a valid ultimate bound of the system, hence $\|x\|_2 \leqslant \sqrt{2} = \text{UB}_2$.

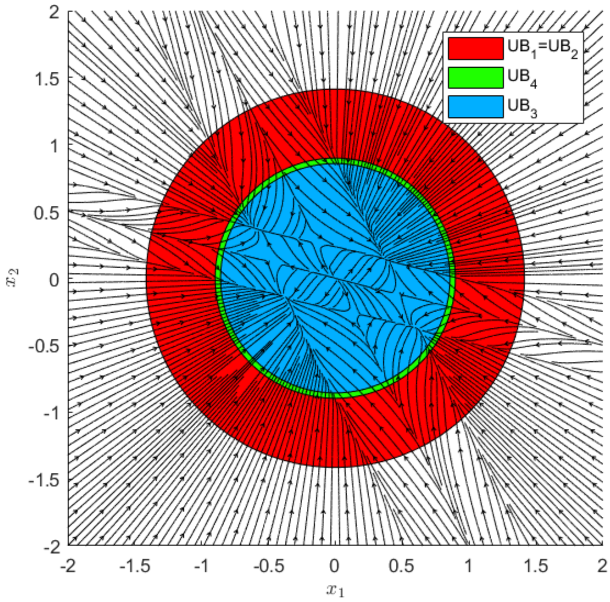

Fig. 4. Ultimate-bounds over the phase space of the closed-loop taken with component-wise nonlinearities

Despite taking into account the link between δ and x, the conservatism introduced by the infinity norm makes $\mathrm{UB}_2 = \mathrm{UB}_1$ for this particular system.

6.2 Orthotopic nonlinearity

Assuming the system is ultimately bounded by $\mathcal{X} = (52)$ (which is verified when h is given by (53)), the ultimate bounds given below also hold in the component-wise case. Theorem 7 now provides the norm of the vertex $\mathcal{V} = \left[\, 5/7 \;\, -3/7 \,\right]^\top$ as a valid ultimate bound, hence $\|x\|_2 \leqslant \frac{6}{7} = \mathrm{UB}_3$. Finally, applying Theorem 8 with

$$Q = \operatorname{diag}(1/2, 1/2), \quad K^\top Q K = \begin{bmatrix} 5/2 & 3 \\ 3 & 17/2 \end{bmatrix}$$

$$\Gamma = \operatorname{diag}\left(11/2 - 3\sqrt{2}, 11/2 + 3\sqrt{2}\right), \quad T_1 = I_2, \quad T_2 = \varnothing$$

$$R = \begin{bmatrix} -\dfrac{1+\sqrt{2}}{\sqrt{4+2\sqrt{2}}} & -\dfrac{1-\sqrt{2}}{\sqrt{4-2\sqrt{2}}} \\ \dfrac{1}{\sqrt{4+2\sqrt{2}}} & \dfrac{1}{\sqrt{4-2\sqrt{2}}} \end{bmatrix}$$

$$r_1 = \frac{\left[W_0\left(\eta\beta(11/2 - 3\sqrt{2})^{\eta/2} r_2^{\eta}\right)/\eta\beta\right]^{\frac{1}{\eta}}}{\sqrt{11/2 - 3\sqrt{2}}}, \quad r_2 = \sqrt{2}e^{\beta}$$

provides the following ultimate bound for all $\beta, \eta > 0$:

$$\|x\|_2 \leqslant \frac{\left[W_0\left(\eta\beta(11/2 - 3\sqrt{2})^{\eta/2} 2^{\frac{\eta}{2}} e^{\eta\beta}\right)/\eta\beta\right]^{\frac{1}{\eta}}}{\sqrt{11/2 - 3\sqrt{2}}}$$

which, evaluated at $\beta = 10^{-3}$ and $\eta = 10^3$ yields $\|x\|_2 \leqslant 0.8973... = \mathrm{UB}_4$.

7. CONCLUSIONS AND PERSPECTIVES

This paper has introduced a novel and unified approach for addressing dead-zone, dead-band, hysteresis and others nonlinear local faults on actuators and sensors of physical system which requires minimal prior knowledge on these faults. Practical ultimate bounds are given for LTI systems. Similarly to the usual dead-zone literature, more robust bounds should be obtainable through adaptive control by leveraging a real-time estimate of the uncertain term introduced in the paper, or by finding sufficient conditions to reduce the assumptions on δ of Section 4.1 to those of Section 4.2. These questions remain open for further investigations.

REFERENCES

Broschart, S. and Scheeres, D.J. (2007). On the implementation of spacecraft hovering under reduced-order dead-band control. In *Journal of Guidance, Control, and Dynamics*.

Ding, D., Cooper, R., and Spaeth, D. (2004). Optimized joystick controller. In *The 26th Annual International Conference of the IEEE Engineering in Medicine and Biology Society*. IEEE. doi:10.1109/iembs.2004.1404350.

Duhem, F. (1897). Die dauernden Aenderungen und die Thermodynamik. *Zeitschrift für Physikalische Chemie*, 24U(1), 666–666. doi:10.1515/zpch-1897-2436.

Gianino, M. (1994). Adaptive control of systems with dead zones. *Master Thesis, Department of Automatic Control - Lund Institute of Technology*.

Goel, M., Maciejewski, A., Balakrishnan, V., and Proctor, R. (2003). Failure tolerant teleoperation of a kinematically redundant manipulator: an experimental study. *IEEE Transactions on Systems, Man, and Cybernetics - Part A: Systems and Humans*, 33(6), 758–765. doi:10.1109/tsmca.2003.818462.

Hassani, V., Tjahjowidodo, T., and Do, T.N. (2014). A survey on hysteresis modeling, identification and control. *Mechanical Systems and Signal Processing*, 49(1-2), 209–233. doi:10.1016/j.ymssp.2014.04.012.

Henrion, D., Tarbouriech, S., and Arzelier, D. (1998). LMI approximations for the radius of the intersection of ellipsoids. In *Proceedings of the 37th IEEE Conference on Decision and Control*. IEEE. doi:10.1109/cdc.1998.758550.

Khalil, H.K. (2014). *Nonlinear Control*. Pearson, Upper Saddle River, NJ.

Preisach, F. (1935). Über die magnetische Nachwirkung. *Zeitschrift für Physik*, 94(5-6), 277–302. doi:10.1007/bf01349418.

Sun, P. and Freund, R.M. (2004). Computation of minimum-volume covering ellipsoids. *Operations Research*, 52(5), 690–706. doi:10.1287/opre.1040.0115.

Tao, G. and Kokotovic, P.V. (1996). *Adaptive control of systems with actuator and sensor nonlinearities*. Adaptive and Cognitive Dynamic Systems: Signal Processing, Learning, Communications and Control. John Wiley & Sons, Nashville, TN.

Tao, G. and Kokotovic, P. (1994). Adaptive control of plants with unknown dead-zones. *IEEE Transactions on Automatic Control*, 39(1), 59–68. doi:10.1109/9.273339.

Tao, G. and Lewis, F.L. (eds.) (2001). *Adaptive control of nonsmooth dynamic systems*. Springer, London, England, 2001 edition.

Zhang, Z., Xu, S., and Zhang, B. (2014). Asymptotic tracking control of uncertain nonlinear systems with unknown actuator nonlinearity. *IEEE Transactions on Automatic Control*, 59(5), 1336–1341. doi:10.1109/tac.2013.2289704.